Viscoelastic Characterization and Modeling of Gelation Kinetics of Injectable In Situ Cross-Linkable Poly(lactide-*co*-ethylene oxide-*co*-fumarate) Hydrogels

Alireza S. Sarvestani, Xuezhong He, and Esmaiel Jabbari*

Biomimetic Materials and Tissue Engineering Laboratories, Department of Chemical Engineering, Swearingen Engineering Center, University of South Carolina, Columbia, South Carolina 29208

Received July 5, 2006; Revised Manuscript Received December 2, 2006

Cell transplantation by injection of biodegradable hydrogels is a recently developed strategy for the treatment of degenerated tissues. A cell carrier should be cytocompatible, have suitable working time and rheological properties for injection, and harden in situ to attain dimensional stability and the desired mechanical strength. Hydrophilic macromer/cross-linker polymerizing systems, due to the relatively high molecular weight of the macromer and its inability to cross the cell membrane, are very attractive as injectable cell carriers. The objective of this research was to determine the effects of cross-linker, initiator, and accelerator concentrations on the gelation kinetics and ultimate modulus of a biodegradable, in situ cross-linkable poly(lactide-*co*-ethylene oxide-*co*-fumarate) (PLEOF) macromer. The in situ polymerizing mixture consisted of PLEOF macromer, methylene bisacrylamide cross-linker, and a neutral redox initiation system of ammonium persulfate initiator and tetramethylethylenediamine accelerator. Measurement of the time evolution of the viscoelastic properties of the network during the sol−gel transition showed the important influence of each component on the gel time and stiffness of the hydrogels. A kinetic model was developed to predict the modulus as a function of composition. Model predictions were consistent with most of the experimental findings. The values of the storage and loss moduli at the gel point were found to be approximately equal for samples with equal PLEOF concentrations, resulting in a simple method to predict the gelation time based on the Winter−Chambon criterion, with the use of the proposed kinetic model. The results of this study can be coupled with component cytocompatibility measurements to predict the effect of composition on the viability of the cells encapsulated in the hydrogel matrix.

Introduction

Injectable biomaterials seeded with cells and growth factors and coupled with minimally invasive arthroscopic techniques are an attractive alternative for treating irregularly shaped degenerated tissues. For example, marrow stromal cells, isolated from the bone marrow, and growth factors can be placed in a supportive hydrogel and injected into an osteochondral defect by an arthroscopic procedure.[1−4] After injection and hardening in situ, the three-dimensional hydrogel matrix guides the organization, differentiation, proliferation, and development of the seeded cells into the desired osteochondral tissue.[5]

A synthetic injectable hydrogel as a cell carrier should satisfy the following criteria.[6,7] The in situ polymerizing mixture should be cytocompatible, have suitable working time and rheological properties for injection via a syringe, and harden in situ to attain dimensional stability and the desired mechanical strength. In addition, the cross-linked hydrogel should degrade into biocompatible molecules in a controlled manner concurrent with tissue regeneration. Hydrophilic macromer/cross-linker polymerizing systems are very attractive as injectable cell carriers. The relatively high molecular weight of the macromer in these systems ($1 \times 10^3-1 \times 10^4$ Da) compared to that of the monomer in monomer/cross-linker systems (<500 Da) significantly diminishes the ability of the macromer to cross the cell membrane and activate intracellular apoptotic pathways. This in turn sharply enhances cytocompatibility of the macromer-based cell carriers.

* Author to whom correspondence should be addressed. Phone: (803) 777-8022. Fax: (803) 777-0973. E-mail: jabbari@engr.sc.edu.

A number of in situ cross-linkable macromers have been developed as cell carriers for tissue regeneration.[8−14] Promising results have been obtained with poly(ethylene glycol) (PEG)-based macromers modified with reactive functional groups such as methacrylate, acrylate, fumarate, and sulfide groups that can be injected and cross-linked in situ using a redox initiator or ultraviolet light to form a hydrogel.[15−19] In an attempt to control water content (hence mechanical strength) and the degradation rate of PEG-based hydrogels, our laboratory has developed a terpolymer of poly(lactide-*co*-ethylene oxide-*co*-fumarate) (PLEOF) consisting of ultralow molecular weight poly(L-lactide) (ULMW PLA) and poly(ethylene oxide) (PEG) blocks linked by unsaturated fumarate units.[20] The PLA and PEG are Food and Drug Administration (FDA)-approved for certain clinical applications, and fumaric acid occurs naturally in the Kreb cycle. The degradation product of ULMW PLA, lactic acid, is resorbed through the metabolic pathways. PEG does not elicit an immune response, and PEG molecular weights less than 5 kDa are excreted by the kidneys. The water content can be adjusted by the ratio of the hydrophilic PEG to hydrophobic PLA blocks and by the molecular weight of PEG. The network mesh size can be controlled by the density of the fumarate groups on the terpolymer chains, and the degradation rate is controlled by the ratio of PLA to PEG blocks in the terpolymer.[21]

The viability of the encapsulated cells in a hydrogel depends on the concentration of the multifunctional cross-linker, initiator, and accelerator and gelation time.[22−25] In addition, the chemical composition and concentration of these components play an important role in controlling the rheological properties and injectability of the hydrogels.[10,26,27] Although significant work

10.1021/bm060648p CCC: $37.00
Published on Web 01/25/2007

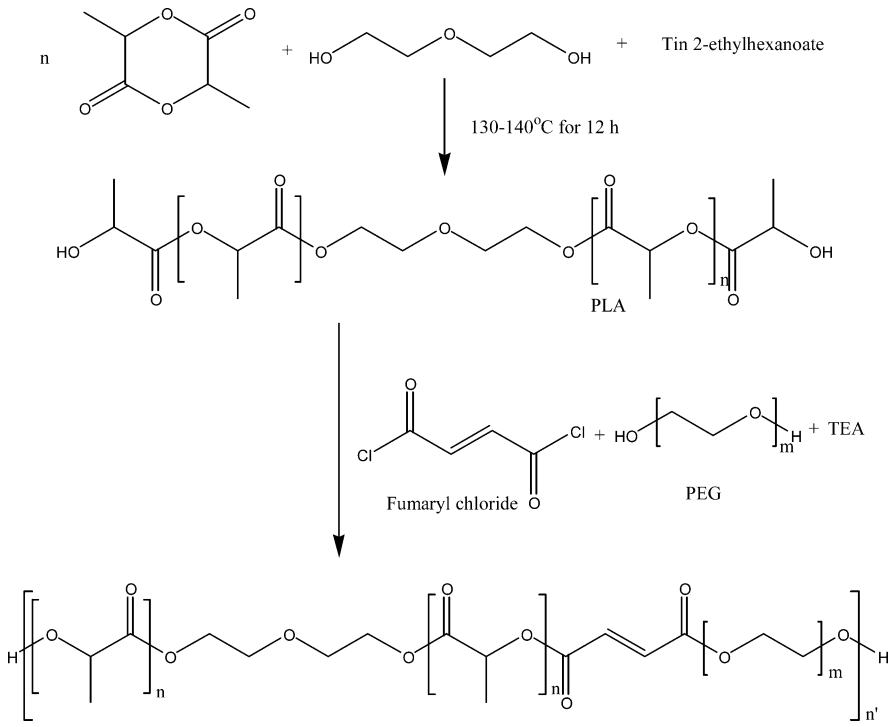

Figure 1. Reaction schemes for the synthesis of the PLEOF macromer.

is done in measuring and modeling the gelation kinetics of monomer/cross-linker hydrogel systems,[28−38] research on the physics of the sol−gel transition and prediction of gelation kinetics of biodegradable in situ cross-linkable macromer/cross-linker hydrogels is scarce.

The objective of this research was to determine experimentally and theoretically the effects of cross-linker, initiator, and accelerator concentrations on the gelation kinetics and ultimate modulus of the in situ cross-linkable PLEOF macromer. The in situ polymerizing mixture consisted of the PLEOF macromer, methylene bisacrylamide (BISAM) cross-linker, and a neutral redox initiation system. Equimolar concentrations of the acidic ammonium persulfate (APS) initiator and basic tetramethylethylenediamine (TEMED) as the radical catalyst were used as the initiation system to have neutral pH during the course of gelation. Measurement of the oscillatory shear modulus was used to continuously monitor the time evolution of the viscoelastic properties of the network during the sol−gel transition and probe the relative influence of each component. On the basis of the experimental results, a kinetic model is developed to predict the elasticity evolution of these systems. The model can predict the elastic modulus of the hydrogel during the cross-linking process as well as the conversion of the BISAM cross-linker, initiator, and unsaturated fumarate groups of the PLEOF macromer. The proposed model also can be used to approximately predict the gelation time of the polymerizing mixture by applying the Winter−Chambon criterion to a linearly viscoelastic cross-linked network at the gel point.[39,40]

Materials and Methods

Synthesis and Characterization of ULMW PLA. ULMW PLA was synthesized by ring-opening polymerization of the L-lactide monomer (LA; Oretc, Inc., Easley, SC) in a dry atmosphere with diethylene glycol (DEG, Aldrich) as the initiator and tin octoate (TOC, Aldrich) as the polymerization catalyst. The molar ratio of DEG to TOC was 25:1, and that of LA to DEG was 10:1. Briefly, 90 g of L-lactide in a three-neck flask was gradually heated in an oil bath to 130 °C under a nitrogen atmosphere. The lactide monomer was allowed to melt for 1 h at 130 °C. Next, 4.5 mL of DEG and 5 mL of TOC were added to the reaction flask with stirring. The polymerization reaction continued for 12 h at 140 °C. The resulting polymer mixture was dissolved in dichloromethane (DCM) and precipitated in ice-cold ether to remove the high molecular weight fraction. After fractionation, ether was removed by rotovaporation, and the polymer was redissolved in DCM and precipitated twice in hexane. The precipitate was dried under vacuum (<5 mmHg) at 40 °C for at least 12 h and stored in a dry atmosphere. The product was characterized by ^{1}H NMR, Fourier transform infrared (FTIR) spectroscopy, and gel permeation chromatography (GPC). The ULMW PLA had M_n and PI values of 1.2 kDa and 1.1 based on GPC, respectively.

Synthesis and Characterization of the PLEOF Terpolymer. PLEOF was synthesized by condensation polymerization of ULMW PLA and poly(ethylene glycol) (PEG; Aldrich) with fumaryl chloride (FuCl; Aldrich). Triethylamine (TEA; Aldrich) was used as the polymerization catalyst (Figure 1). FuCl was purified by distillation at 161 °C, and PEG was dried by azeotropic distillation from toluene. The molar ratios of FuCl/(PEG + PLA) and TEA/(PEG + PLA) were 0.9:1.0 and 1.8:1.0, respectively. The weight ratio of PEG to PLA was 70:30 to produce a hydrophilic water-soluble terpolymer. In a typical reaction, 14.0 g of PEG and 6.0 g of ULMW PLA were dried by azeotropic distillation from toluene and then dissolved in 150 mL of DCM under a dry nitrogen atmosphere in a three-neck reaction flask in an ice bath. Next, 0.61 mL of FuCl and 1.55 mL of TEA, each dissolved in 30 mL of DCM, were added dropwise to the reaction with stirring. The reaction proceeded for 6 h in an ice bath and continued for 12 h under ambient conditions. After completion of the reaction, the solvent was removed by rotovaporation, the residue was dissolved in 100 mL of anhydrous ethyl acetate to precipitate the byproduct triethylamine hydrochloride, and the salt was removed by filtration. Ethyl acetate was removed by rotovaporation. The macromer was redissolved in DCM and precipitated twice in cold ethyl ether. It was dried in vacuum (<5 mmHg) at ambient temperature for at least 12 h and stored at −20 °C.

The structure of the PLEOF macromer was characterized by ^{1}H NMR and FTIR. Four singlet chemical shifts with peak positions at 1.6, 3.5, 6.8, and 6.9 ppm, two triplets with peaks positions at 3.6 and 4.2 ppm,

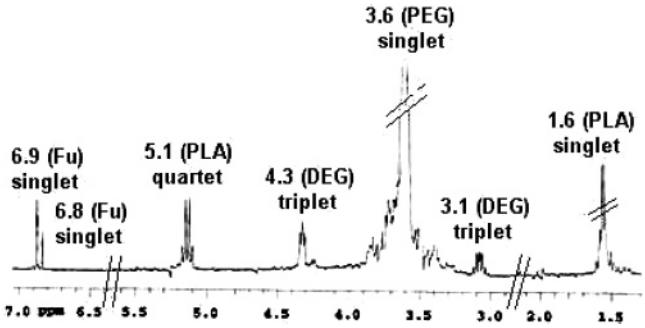

Figure 2. ^{1}H NMR spectrum of the PLEOF terpolymer.

and a quartet with peak position at 5.1 ppm were observed in the ^{1}H NMR spectrum of the terpolymer (Figure 2). The singlet chemical shift with a peak position at 1.6 ppm was attributed to the hydrogens of the methyl group ($-CH_3$) of the lactide monomer. The singlet chemical shift at 3.5 ppm was attributed to the methylene hydrogens (CH_2-CH_2-O-) of the ethylene oxide repeat units. The triplet chemical shifts centered at 3.6 and 4.2 ppm were due to the hydrogens of the methylene groups attached to the ether group ($-CH_2-O-CH_2-$) and the methylene groups attached to the ester group of the lactide (CH_2-OOC-), respectively, on the initiator DEG. The quartet chemical shift with a peak position at 5.1 ppm was due to the hydrogen attached to the methine group of the lactide monomer. The singlet shifts at 6.90 and 6.95 ppm were attributed to the methine hydrogens of the fumarate in the middle of the chain ($-OOC-CH=CH-COO-$) and on the chain ends ($-OOC-CH=CH-COOH$), respectively. The presence of the peaks at 6.90 ppm in the NMR spectrum attributable to the hydrogens of the fumarate group and the presence of a band due to the ester carbonyl stretching vibration centered at 1725 cm^{-1} in the FTIR spectra confirmed the incorporation of fumarate monomers into the PLEOF macromer. The PLEOF macromer with PLA and PEG molecular weights of 1.2 kDa (PI of 1.1) and 3.4 kDa (PI of 1.1) had M_n and PI values of 10.5 kDa and 1.7, respectively, as determined by GPC.

Hydrogel Preparation. Hydrogels were prepared by radical polymerization of the PLEOF macromer with BISAM as the cross-linking agent and a redox initiation system in aqueous solution. The redox initiation system consisted of APS and TEMED with equimolar concentrations in the range of 0.005−0.02 M. Equimolar concentrations of initiator and accelerator were used to keep the pH of the polymerization mixture constant at 7.4. PLEOF hydrogels without BISAM cross-linker were also prepared to serve as the controls. Briefly, BISAM cross-linker (final concentration in the range of 0−0.25 M) was dissolved in 0.825 mL of distilled deionized water (DDI) water by heating the mixture to 50 °C. Next, 315 mg of PLEOF macromer was added to the BISAM solution, and the mixture was heated to aid dissolution. The mixture was vortexed periodically to completely dissolve the macromer. Then, 105 μL of APS and TEMED (0−0.2 M initial concentration) were added to initiate the polymerization. The mixture was mixed vigorously for 20 s before measuring the gelation kinetics by rheometry.

The following nomenclature is used to identify the concentration of cross-linker and initiator/accelerator in various hydrogel samples. Hydrogels prepared with the PLEOF macromer are specified by the symbol "P-*m* B-*n* I/A" where *m* and *n* represent the final molar concentrations of BISAM and APS/TEMED, respectively. Hydrogels prepared without PLEOF are specified by "*m* B-*n* I/A" without the letter "P".

Gelation Kinetics and Rheological Measurements. The time for the onset of gelation and the evolution of elasticity was determined by rheometry at a constant temperature of 37 °C in a constant strain mode. The measurements were obtained with an AR-2000 rheometer (TA Instruments, New Castle, DE) using a parallel plate geometry (20 mm diameter). The polymerizing mixture was injected on the Peltier plate, and the upper geometry was lowered to a gap of 500 μm. The elapsed time between mixing/injection and start of the data collection was 30 s for all experiments.

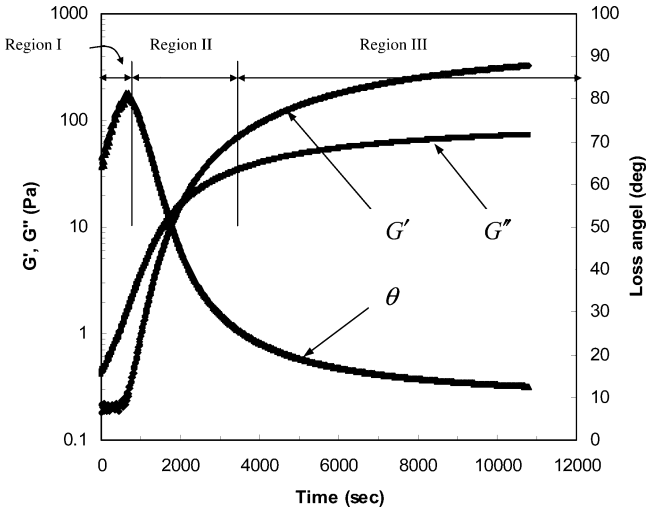

Figure 3. Evolution of the viscoleastic properties of P-0.05 B-0.005 I/A with time.

A sinusoidal shear strain profile was exerted on the sample via the upper plate, and the force required to strain the sample was monitored as a function of time. The deformation amplitude was 1% to remain within the linear region of viscoelasticity. The time sweep oscillatory shear measurements were done at a constant frequency of 1 Hz for 3 h. Each measurement was immediately followed by a frequency sweep in the range from 0.1 to 10 Hz. The geometry was covered with a humidity chamber to prevent dehydration during the experiment. Here, we report storage moduli (G'), loss moduli (G''), and the phase angles ($\theta = \tan^{-1}(G''/G')$) of the samples during the gelation process. Each experiment was repeated three times to obtain the mean and standard deviation.

Experimental Results

General Observations. Two measurements were performed for each sample: a time sweep measurement in which the storage and loss moduli were monitored as a function of time and a steady-state frequency sweep at low strain amplitude. From the time sweep experiments, the rate and extent of cross-linking were determined. The subsequent frequency sweep was used to verify the formation of a chemically cross-linked gel. Frequency independence of the storage modulus confirms that the gels are cross-linked and mechanically robust, while samples with higher sol fractions and longer relaxation times exhibit a dependence on frequency.

Figure 3 shows the time dependence of G', G'', and θ for the sample P-0.05 B-0.005 I/A. Other hydrogels exhibited similar gelation curves. A shift from a predominantly viscous liquid ($G'' > G'$) to a strongly viscoelastic solidlike material ($G' > G''$) was observed. The corresponding time of crossover from a viscous behavior to an elastic response (i.e., the time at which $G' = G''$) was regarded as the gel time.[39,40]

Three main regions can be distinguished in the time sweep curves during the course of the reaction (Figure 3). First, a short induction period is observed, where G' and G'' do not change appreciably with time. The duration of the induction period was affected by the concentrations of initiator/accelerator and cross-linker and approached zero at high concentrations of these components. Inhibition of the primary free radicals by oxygen present in the polymerizing mixture may also affect the duration of the induction regime. In the second region, the network structure began to form, and the elastic modulus increased

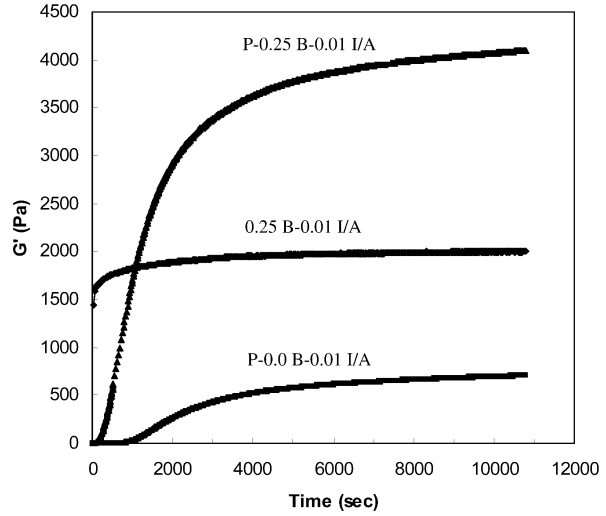

Figure 4. Comparison of the evolution of the storage modulus for sample P-0.25 B-0.01 I/A with those of samples without the PLEOF macromer (0.25 B-0.01 I/A) and without the BISAM cross-linker (P-0.0 B-0.01 I/A).

sharply and monotonically with time. This was followed by the final phase, where the slope of the G' curve versus time continuously decreased, inferring that the network formation process was reaching completion. The loss modulus reached a plateau value faster than the storage modulus, and its ultimate magnitude was negligible compared to the corresponding storage plateau modulus.

The neat BISAM polymerizing mixture (without the addition of PLEOF) cross-linked almost immediately after the addition of initiator and accelerator in the range of concentrations studied (0.05−0.25 M). In addition, cross-linked BISAM chains precipitated from the solution giving rise to an inhomogeneous nontransparent gel. This well-known behavior of bisacrylamide gels has been attributed to the domination of intramolecular cyclization, formation of microgels prior to the onset of macrogelation, and eventually inhomogeneous distribution of monomers.[34,37,38] As the reaction proceeds, microgels are connected to the macrogel through their peripheral pendent vinyl groups, whereas those vinyl groups in the microgel's interior remain unreacted.

Notably, after the addition of the PLEOF macromer, the polymerizing mixture cross-linked to a homogeneous and transparent hydrogel. This implied that the fumarate groups of the PLEOF chains cross-reacted primarily with the primary BISAM chains, as opposed to reacting with fumarate groups on other PLEOF chains, and the higher solubility of the PLEOF macromer in the aqueous solution (due to the PEG blocks) increased the solubility of the entire polymerizing mixture.

This hypothesis is verified by comparing the time sweep results for P-0.25 B-0.01 I/A with those of the neat BISAM (0.25 B-0.01 I/A) and neat PLEOF (P-0.0 B-0.01 I/A), as shown in Figure 4. The PLEOF/BISAM cross-linked gel (PLEOF concentration $\approx$ 0.04 M) showed a significantly higher ultimate modulus compared to that of the neat PLEOF or BISAM cross-linked gels. According to the theory of rubber elasticity,[41] the storage modulus of a permanently cross-linked gel is linearly proportional to the number density of the elastically active cross-link points N_e; i.e.,

$$G' \sim N_e \tag{1}$$

In the neat BISAM gel (0.25 B-0.01 I/A) a significant fraction of the BISAM cross-links participate in the formation of just one cluster corresponding to only one active network junction,[34,38] as shown by Figure 5a. However, for a constant BISAM concentration, the higher storage modulus of the homogeneous and transparent P-0.25 B-0.01 I/A can be attributed to the higher density of the pendent BISAM vinyl groups, which are converted to elastically active cross-links due to network homogeneity (Figure 5b).

The process of the PLEOF/BISAM cross-linking reaction can be assumed as follows. The system is initially comprised of homogeneously dissolved PLEOF chains and BISAM cross-linker. Upon the addition of initiator and accelerator, BISAM reacts with primary radicals to form short chains. Next, these growing primary radicals react with the fumarate groups on the PLEOF and form BISAM-grafted PLEOF chains. The lower mobility of the PLEOF macromers compared to that of primary

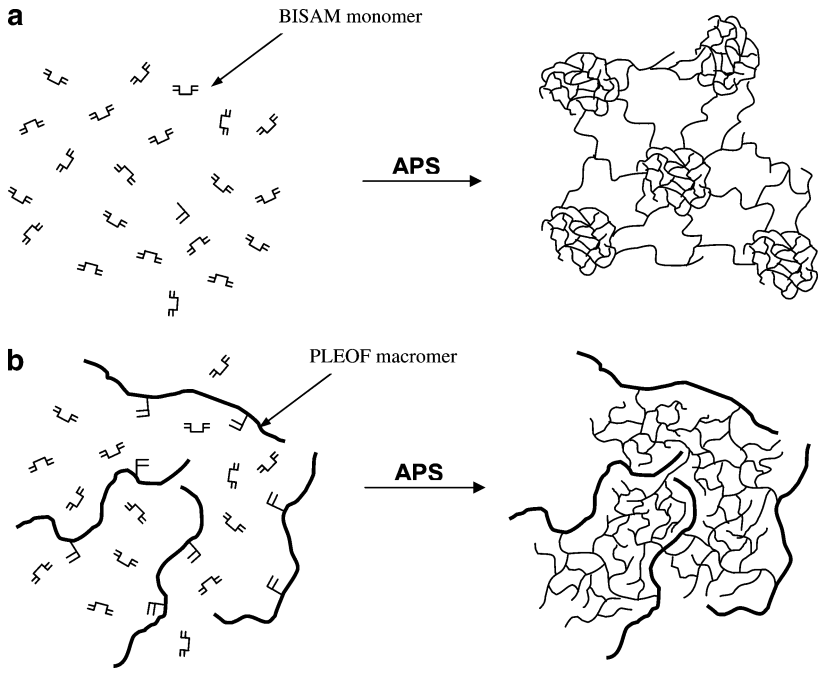

Figure 5. Schematic representation of the microstructure of (a) BISAM and (b) PLEOF/BISAM hydrogels.

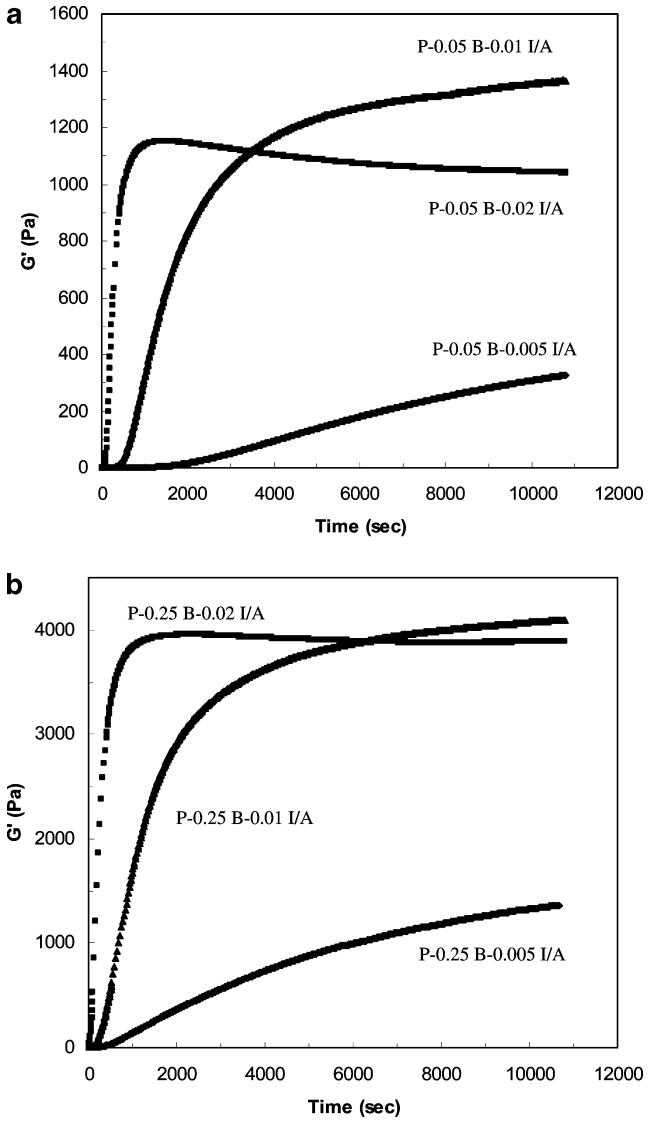

Figure 6. Effects of the concentration of APS/TEMED on the time evolution of the storage moduli of (a) P-0.05 B and (b) P-0.25 B hydrogels.

BISAM chains restricts direct interaction and reaction between the fumarate groups on different PLEOF chains, but the PLEOF chains are connected remotely through the primary BISAM chains. For the PLEOF/BISAM polymerizing mixture, the modulus continues to increase in the terminal phase of the gelation due to local scale structural rearrangement of the primary BISAM chains and their reactions with pendent double bonds.

Effects of Initiator and Accelerator. The effects of APS/TEMED concentration on the gelation kinetics of P-0.05 B and P-0.25 B are shown in Figures 6a and 6b, respectively. The corresponding gel times are also shown in Figures 7a and 7b. The rate of cross-linking and the gelation time were strongly dependent on the concentrations of the initiator and accelerator. At 0.02 M initiator concentration, the ultimate storage modulus was lower than that of the 0.01 M initiator concentration. This can be explained by intramolecular cross-linking (i.e., cyclization) of the vinyl groups of the primary BISAM chains, resulting in reduction of the elastically active cross-link points in the gel.

The frequency sweep experiments on P-0.10 B with various amounts of initiator/accelerator are shown in Figure 8. Samples with other BISAM concentrations showed qualitatively similar behaviors. At high APS concentrations, the modulus was

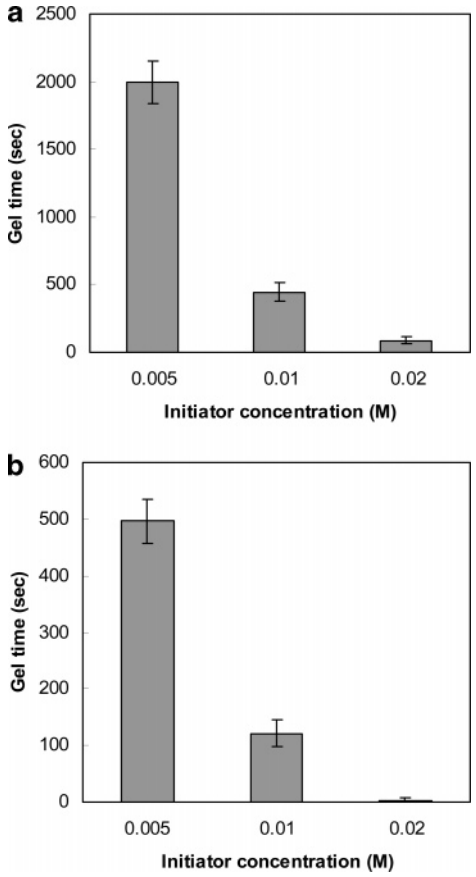

Figure 7. Effects of the concentration of APS/TEMED on the gelation time of (a) P-0.05 B and (b) P-0.25 B hydrogels.

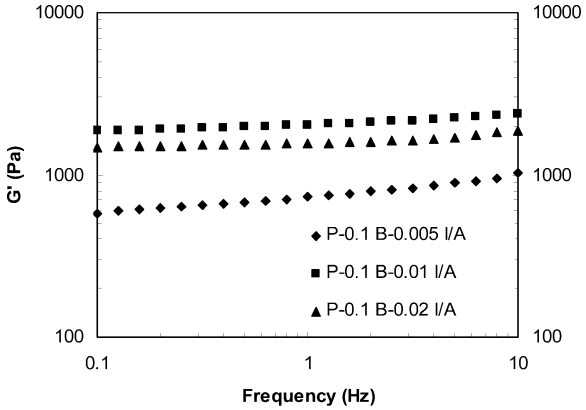

Figure 8. Effects of the concentration of APS/TEMED on the frequency sweep response of the P-0.1 B hydrogel.

independent of frequency, confirming that the gels were thoroughly cross-linked with insignificant sol fraction. At low APS concentrations (0.005 M), the modulus showed a weak dependence on frequency that can be attributed to longer relaxation times in the system arising from the sol fraction (i.e., PLEOF or BISAM chains that are not connected to the network) or long dangling BISAM chains. These results demonstrate that at low APS concentrations, due to insufficient concentrations of radicals, the BISAM chains were not completely integrated into the PLEOF/BISAM network.

Effects of BISAM Concentration. Figure 9 shows the elasticity evolution of the PLEOF hydrogels with different BISAM concentrations at a constant APS/TEMED concentration of 0.1 M. A significant increase in the elastic modulus and a decrease in the gelation time were observed with increasing

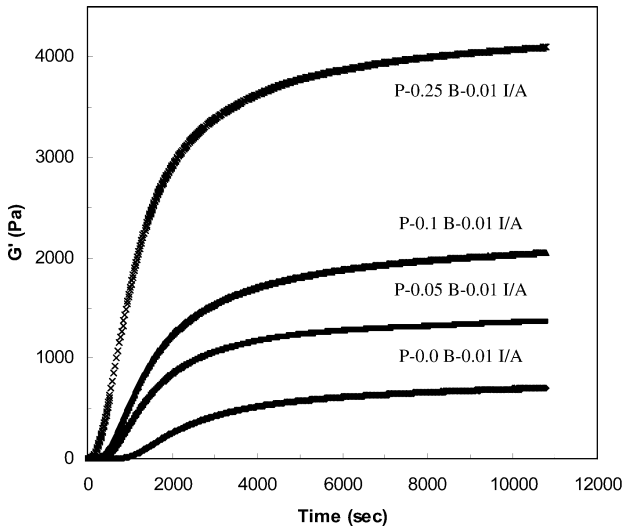

Figure 9. Effects of the BISAM concentration on the time evolution of the storage modulus of the P-0.01 I/A hydrogel.

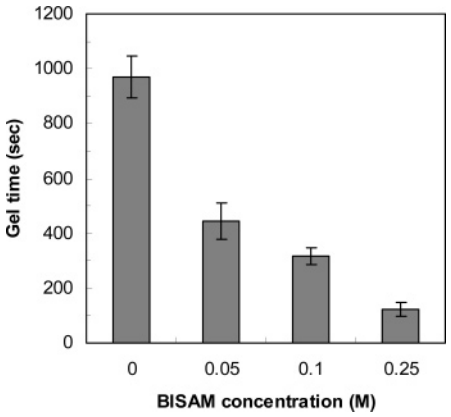

Figure 10. Effects of the BISAM concentration on the gelation time of the P-0.01 I/A hydrogel.

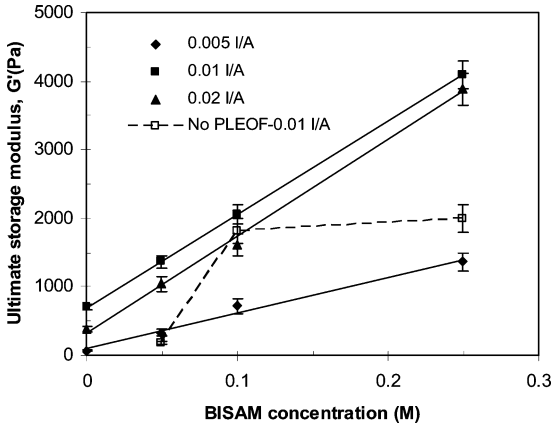

Figure 11. Effects of the BISAM concentration on the ultimate storage moduli of hydrogels with (solid lines) and without (dashed line) PLEOF after 3 h for different concentrations of APS/TEMED.

cross-linker concentration (Figure 10), indicating that the cross-linker affected the rate of polymerization and formation of the network.

The values of the storage moduli after 3 h for the hydrogels with different BISAM concentrations are plotted in Figure 11. The figure also includes the results from hydrogels prepared only with BISAM (dashed line). For the case with no PLEOF, the results show an increase in the ultimate storage modulus with BISAM concentration followed by a plateau at higher

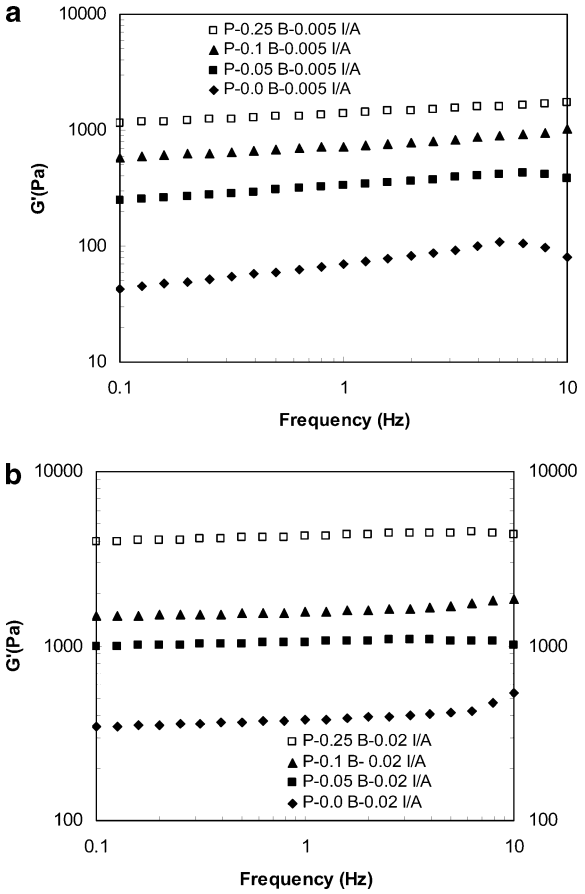

Figure 12. Effects of BISAM concentration on the frequency sweep response of (a) P-0.005 I/A and (b) P-0.02 I/A hydrogels.

cross-linker concentrations. This property of the acrylamide gels is generally explained by the presence of heterogeneities in the gel (Figure 5a).[29,34,38] In hydrogels prepared with the PLEOF macromer, G' followed a linear relationship with cross-linker concentration and increased continuously with increasing BISAM concentration within the entire range of concentrations investigated. The continuous increase in modulus with increasing BISAM concentrations again confirmed that the gel in the presence of PLEOF had a more homogeneous microscopic structure.

Figures 12a and 12b show a representative frequency spectrum for P-0.005 I/A and P-0.02 I/A compositions with different BISAM concentrations. At high initiator concentrations, the material was completely elastic, and the storage modulus was independent of frequency for all BISAM concentrations. However, at low initiator concentrations, the rheological spectrum exhibited a slight frequency dependence, increasing with reduction of the BISAM concentration. Again, this can be attributed to longer relaxation times in the system arising from the sol fraction or long dangling chains.

Influence of Composition on the Gel Point. The viscoelastic characteristics of an incipient gel is often described by the model of Winter and Chambon who proposed a power law equation for the storage and loss moduli at the gelation time[39,40]

$$G'_{gel}(\omega) = G''_{gel}(\omega) = A\omega^{\alpha} \qquad (2)$$

where A is a material constant. Winter and Chambon hypothesized that such a power law relation is valid in the entire range of frequency. On this basis, the Kramers−Kronig relation gives $\alpha = {}^{1}/_{2}$ as the only possible value for the exponent.

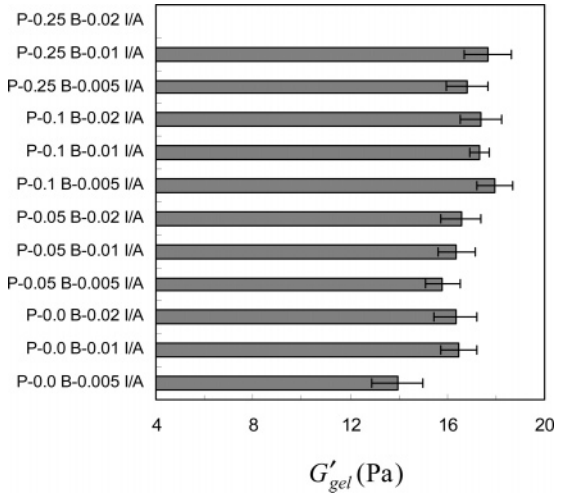

Figure 13. Storage (and loss) modulus of the hydrogels at the gel point.

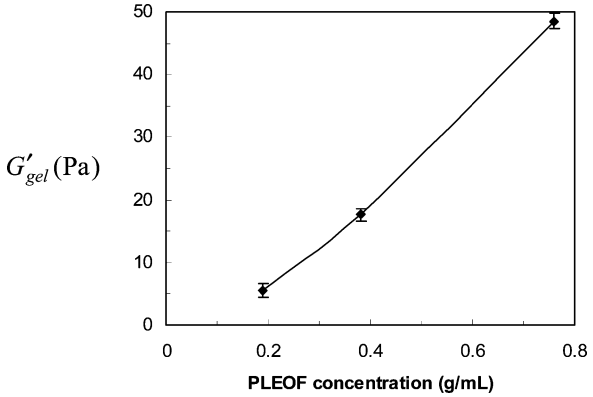

Figure 14. Gel point storage moduli of the hydrogels with different concentrations of PLEOF. Concentrations of BISAM and APS/TEMED were constant at 0.25 M and 0.01 M, respectively.

The corresponding values of the storage (and loss) modulus at the crossover point are shown in Figure 13. For P-0.25 B-0.02 I/A, the gelation point was not recorded because it happened before the start of data collection by the rheometer. Notably, all of the samples showed an almost equal storage modulus of 16.86 ± 0.68 Pa at the onset of gelation. Hence, it can be deduced that the material constant A in eq 2 is weakly affected by the concentrations of the cross-linker and initiator/accelerator. The polymerizing mixture P-0.0 B-0.005 I/A with the minimum capability for networking due to the lack of a cross-linking agent and the lowest concentration of the initiator was an exceptional case with $G'_{gel} < 16.86$Pa.

To test the effect of PLEOF concentration on the elastic and loss moduli at the gel point, time sweep experiments were conducted with different PLEOF concentrations (at constant cross-linker and initiator/accelerator concentrations), and the results are shown in Figure 14. These results clearly show that G'_{gel} increased monotonically with the concentration of PLEOF and confirmed that the material constant A in eq 2 is controlled only by the concentration of the macromer. The independence of the storage modulus from the concentrations of BISAM and APS/TEMED at the gel point provides a method to predict the gel time that will be discussed in the next section.

Kinetic Model for Gelation

Application of the in situ cross-linkable PLEOF gels as cell and growth factor carriers in tissue regeneration requires a priori prediction of the gelation time, sol fraction, and modulus as a function of composition. This ideally allows optimization of the hydrogel composition prior to any chemical synthesis and cell encapsulation. To this end, in this section, a kinetic model is proposed to predict the properties of the network as a function of time after injection under isothermal conditions. The model is based on the following assumptions:

1. In the presence of the PLEOF macromer, the polymerization system remains soluble in the aqueous solution during the course of gelation.
2. Reactions between the BISAM primary chains are not diffusion-controlled.
3. Intramolecular cross-linking by cyclization of the primary BISAM chains is not considered.
4. The reactivity of the growing BISAM chains depends only on the reactivity of the terminal unit.
5. Terminal double bonds formed by chain transfer or termination reactions are assumed to behave similar to pendent double bonds.
6. PLEOF and BISAM chains mutually contribute to stress production, and the network stiffness is directly proportional to the number density of their elastically active cross-link points.
7. The volume change due to changes in the network density during cross-linking is not considered.

It is assumed that the gelation process consists of initiation, propagation, chain transfer to the polymer, and termination by disproportionation. These elementary reactions are listed below.

Initiation

$$I \xrightarrow{k_d} {}^2R^* \tag{3a}$$

$$R^* + B \xrightarrow{k_{iB}} B_1 \tag{3b}$$

$$R^* + \mathrm{PDB^F} \xrightarrow{k_{if}} F^* \tag{3c}$$

Propagation

$$B_n + B \xrightarrow{k_{pB}} B_{n+1} + \mathrm{PDB^B} \tag{4}$$

Cross-linking

$$B_n + \mathrm{PDB^B} \xrightarrow{k_{xB}} X^B + \mathrm{PDB^B} \tag{5a}$$

$$B_n + \mathrm{PDB^F} \xrightarrow{k_{xF}} X^F + \mathrm{PDB^B} \tag{5b}$$

Transfer to monomer

$$B_n + B \xrightarrow{k_{fB}} B_1 + D_n + {}^2\mathrm{PDB^B} \tag{6}$$

Termination by disproportionation

$$B_n + B_r \xrightarrow{k_{tdB}} D_n + D_r + {}^3\mathrm{PDB^B} \tag{7a}$$

$$B_n + F^* \xrightarrow{k_{tdF}} D_n + \mathrm{PDB^F} + \mathrm{PDB^B} \tag{7b}$$

Here, I, B, $\mathrm{PDB^F}$, and $\mathrm{PDB^B}$ represent the molar concentrations of APS, BISAM monomer, double bonds of the fumarate groups on PLEOF, and the pendent double bonds on the radical BISAM chains, respectively. Moreover, R^* and F^* refer to the concentrations of primary radicals and those fumarate groups that reacted with the primary radicals, respectively. The concentration of radical BISAM chains with n units is shown by B_n, while that of the dead chains is represented by D_n. Polymer radicals

can interact with pendent double bonds on BISAM chains and form branch points with concentration X^B. Growing BISAM radicals can also react with fumarate double bonds and form cross-links (X^F).

To predict the time-dependent concentration of the reactant species, first we define the *i*th moment of the molecular weight distribution of the radical BISAM chains as

$$M_i = \sum_{n=1}^{\infty} n^i B_n \tag{8}$$

Consequently, the following rate equations can be derived from the elementary reactions given by eqs 3−7

$$\frac{dR^*}{dt} = 2k_d I - k_{iB} R^* B - k_{iF} R^* \mathrm{PDB}^F \tag{9}$$

$$\frac{dB}{dt} = -k_{iB} R^* B - k_{pB} B M_0 - k_{fB} B M_0 \tag{10}$$

$$\frac{d\mathrm{PDB}^F}{dt} = -k_{iF} R^* \mathrm{PDB}^F - k_{xF} \mathrm{PDB}^F M_0 + k_{tdF} F^* M_0 \tag{11}$$

$$\frac{dF^*}{dt} = k_{iF} R^* \mathrm{PDB}^F - k_{tdF} F^* M_0 \tag{12}$$

$$\frac{d\mathrm{PDB}^B}{dt} = k_{pB} B M_0 + k_{xF} \mathrm{PDB}^F M_0 + 2k_{fB} B M_0 + 3k_{tdB} M_0^2 + k_{tdF} F^* M_0 \tag{13}$$

$$\frac{dX^B}{dt} = k_{xB} \mathrm{PDB}^B M_0 \tag{14}$$

$$\frac{dX^F}{dt} = k_{xF} \mathrm{PDB}^F M_0 \tag{15}$$

The rates of change of the zero, first, and second moments of B_n with time can be represented by the following ordinary differential equations

$$\frac{dM_0}{dt} = -k_{xB} \mathrm{PDB}^B M_0 - k_{xF} \mathrm{PDB}^F M_0 - k_{fB} B M_0 - k_{tdB} M_0^2 - k_{tdF} F^* M_0 \tag{16a}$$

$$\frac{dM_1}{dt} = k_{pB} B M_0 - k_{xB} \mathrm{PDB}^B M_1 - k_{xF} \mathrm{PDB}^F M_1 - k_{fB} B M_1 - k_{tdB} M_0 M_1 - k_{tdF} F^* M_1 \tag{16b}$$

$$\frac{dM_2}{dt} = 2k_{pB} B M_1 + k_{pB} B M_0 - k_{xB} \mathrm{PDB}^B M_2 - k_{xF} \mathrm{PDB}^F M_2 - k_{fB} B M_2 - k_{tdB} M_0 M_2 - k_{tdF} F^* M_2 \tag{16c}$$

Using the theory of rubber elasticity for phantom networks, the elasticity of the system is assumed to be proportional to the number density of the effective cross-link points in the network; i.e., $G'(t) = C^B X^B(t) + C^F X^F(t)$ where C^B and C^F are temperature-dependent coefficients representing the fractions of cross-links that are elastically active.[41] For the sake of simplicity, these temperature-dependent coefficients are assumed to remain constant during the course of gelation.

Discussion. The set of ordinary differential equations given in eqs 9−16 can be solved numerically. In this section, the model predictions are compared with the experimental results (Figures 15a−c). The values of the kinetic rate constants in eqs 3−7 are presented in Table 1. The rate constants for the reaction of acrylamide groups between the BISAM chains (BISAM

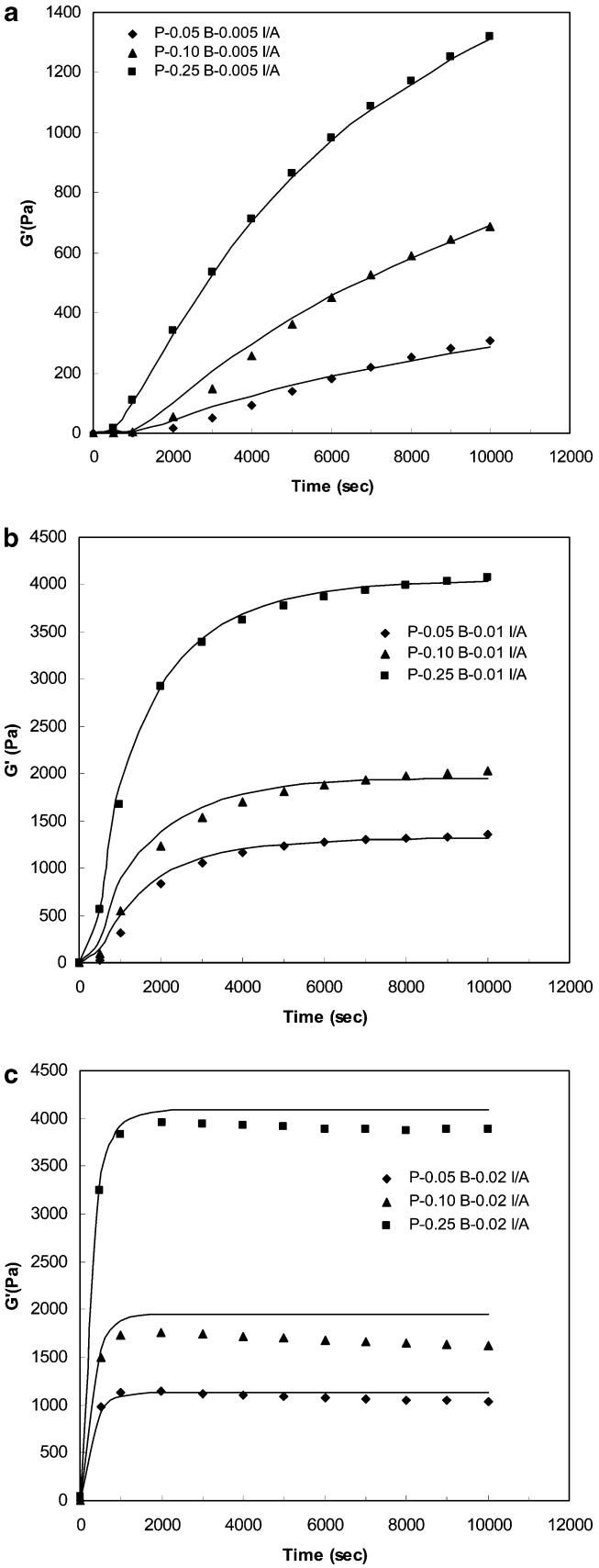

Figure 15. Comparison of the model predictions and experimental data for the elasticity evolution of (a) P-0.005 I/A, (b) P-0.01 I/A, and (c) P-0.02 I/A hydrogels prepared with various concentrations of the BISAM cross-linker.

Table 1. Kinetic Rate Constants for the Cross-Linking of PLEOF/BISAM Polymerizing Mixtures[a]

constant	value (L/(M s))
k_iB	$\sim 1 \times 10^{10}$
k_iF	$\sim k_iB$
k_pB	$1.65 \times 10^6 \exp(-2743/RT)$
k_xB	k_pB
k_xF	$\sim 10^{-2} k_pB$
k_fB	$9.55 \times 10^6 \exp(-10\ 438/RT)$
$k_{td}B$	$(1532 \exp(-741/RT))^2$
$k_{td}F$	$\sim 10^{-2} k_{pB}$

[a] R is the gas constant and T represents the absolute temperature.

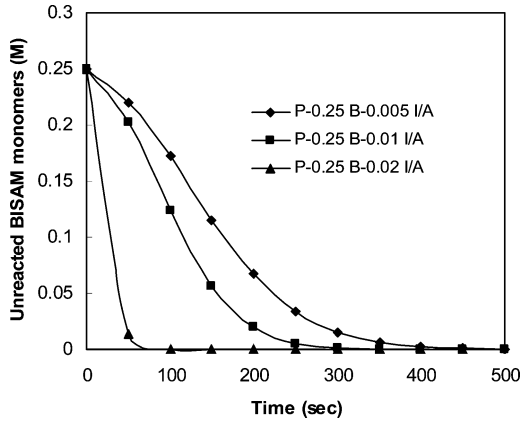

Figure 16. Effects of APS/TEMED concentration on the concentration of unreacted BISAM versus time.

homopolymerization) were taken from ref 37 while the rate constants for the reaction of acrylamide groups on BISAM and fumarate groups on PLEOF chains (PLEOF/BISAM reactions) were obtained by the best fit of the experimental time sweep data to the proposed kinetic model. Likewise, the value of $k_d \approx 10^{-3}$ s^{-1} for the APS dissociation rate in the presence of TEMED was obtained from the best fit. All adjustable parameters were evaluated by fitting the model predictions to the time sweep measurements of the P-0.25 B-0.005 A/I sample.

From the extracted parameters it is evident that the rate of reaction between acrylamide groups of BISAM and fumarate groups of PLEOF was significantly less than that of acrylamide groups between two BISAM chains. This can be explained by the lower reactivity of the fumarate double bond (secondary unsaturated bond) versus that of acrylamide (primary double bond) and the lower mobility of the fumarates on the longer PLEOF chains. Because of the lower reactivity of the fumarate groups, it was assumed that the fumarate groups can only be linked indirectly through the more reactive radical BISAM chains.

There is a reasonable agreement between the experimental results and model predictions except for systems with high concentrations of APS/TEMED (0.02 M). This discrepancy can be explained by the higher probability of intramolecular cross-linking reactions (i.e., cyclization) at higher APS/TEMED concentrations (two or more radicals on the same growing chain), which was not included in the proposed kinetic model.

The model predictions for the concentration of unreacted BISAM versus time are shown in Figure 16. As expected, the concentration of initiator/accelerator has a dramatic effect on the rate of BISAM conversion. The viability of the cells encapsulated in the polymerizing matrix depends on the concentrations of the unreacted low molecular weight compounds in the mixture, such as BISAM.[25] Therefore, prediction of the time evolution of the concentration of unreacted BISAM can indirectly provide information about cell viability during the course of cross-linking.

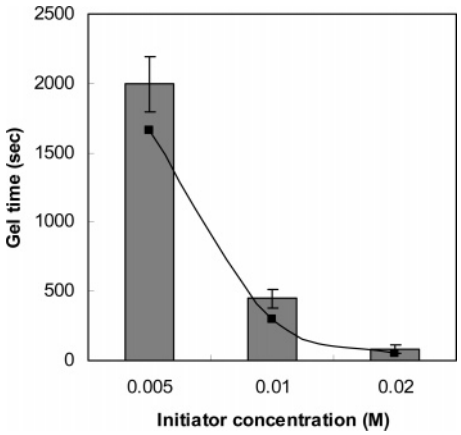

Figure 17. Comparison of the model predictions (solid line) and experimental measurements for the gel point for the P-0.1 B sample at different APS/TEMED concentrations.

The predicted evolution of the storage modulus, shown in Figure 15, can also be used to estimate the gelation time of the samples. As the experimental results show, the value of the storage modulus at the gel point is mainly affected by the concentration of the PLEOF macromer and is independent of the initiator and cross-linker concentrations. For the PLEOF concentration investigated in this work (0.04 M), the value of the storage modulus at the gel point was ~16.86 Pa, independent of the BISAM and APS/TEMED concentrations. Hence, the time corresponding to the modulus of ~16.86 Pa on the storage modulus versus time curves is the gel time of each sample. The predicted gel times of the sample P-0.1 B for different APS/TEMED concentrations are shown in Figure 17.

While the predicted gel times follow the trend of the experimentally measured values, the model consistently underestimated the actual time for gelation. The reason is that the proposed model for elasticity evolution overestimates the value of the storage modulus at the early stages of the reaction. In fact, the duration of the actual induction time (i.e., phase I of the cross-linking reaction) was longer than what the model predicted for all samples. One reason for such a discrepancy could be the effect of the residual oxygen in the polymerizing mixture. In fact oxygen could act as a radical scavenger, suppress the polymerization reaction, and increase the induction time until it is consumed.[42]

Conclusions

The gelation kinetics of the poly(lactide-*co*-ethylene oxide-*co*-fumarate) (PLEOF) macromer was investigated using rheological monitoring. The in situ polymerizing mixture consisted of the PLEOF macromer, methylene bisacrylamide (BISAM) cross-linker, and a neutral redox initiation system. The time evolution of the network during the sol−gel transition was continuously monitored by measurement of the viscoelastic properties throughout the in situ cross-linking (in the rheometer). The effects of the cross-linker and initiator/accelerator concentrations on the elasticity evolution of the system were determined. The following conclusions are made on the basis of the experimental observations:

(1) The rate of cross-linking and the gelation time were strongly dependent on the concentrations of the initiator and

accelerator. The ultimate storage modulus of the hydrogels was enhanced with an increase in APS/TEMED concentrations. However, this trend was reversed at very high initiator concentrations (0.02 M), possibly due to the cyclization effect.

(2) The shear moduli of the hydrogels with a low concentration of APS/TEMED (0.005 M) showed frequency dependence, evidence for the existence of the sol fraction or long dangling chains with longer relaxation times. At higher concentrations of initiator/accelerator, the gel response was frequency-independent, characteristic of a well-developed cross-linked polymer network.

(3) As the concentration of the cross-linker was increased, the crossover from viscous to elastic behavior occurred at an earlier time. The ultimate modulus of the gels was found to increase linearly with the cross-linker concentration.

(4) The storage and loss moduli of the polymerizing mixture at the gel point were found to be independent of the concentration of initiator and cross-linker but strongly dependent on the concentration of the PLEOF macromer.

On the basis of the experimental results, the network structure was assumed to consist of PLEOF chains cross-linked through the fumarate groups by BISAM chains, homogeneously distributed in the solution. A kinetic model was developed to predict the effect of composition on hydrogel elasticity and the conversion rate of cross-linking constituents. From the estimated time sweep curves, the time corresponding to the experimentally measured G'_{gel} (approximately common value for all samples) can be regarded as the gel time of that hydrogel.

Acknowledgment. This work was supported by grants from the Arbeitsgemeinschaft Fur Osteosynthesefragen Foundation, the Aircast Foundation, and the Office of Research and Health Sciences at the University of South Carolina.

References and Notes

(1) Vacanti, C. A.; Langer, R.; Schloo, B.; Vacanti, J. P. *Plast. Reconstr.. Surg.* **1991**, *88*, 753.
(2) Peppas, N. A.; Langer, R. *Science* **1994**, *263*, 1715.
(3) Caplan, A. I.; Elyaderani, M.; Mochizuki, Y.; Wakitani, Y. S.; Goldberg, V. M. *Clin. Orthop. Relat. Res.* **1997**, *342*, 254.
(4) Temenoff, J. S.; Mikos, A. G. *Biomaterials* **2000**, *21*, 431.
(5) Hangody, L.; Kish, G.; Karpati, Z.; Udvarhelyi, I.; Szigeti, I.; Bely, M. *Orthopedics* **1998**, *21*, 751.
(6) Hou, Q.; De Bank, P. A.; Shakesheff, K. M. *J. Mater. Chem.* **2004**, *14*, 1915.
(7) Jabbari, E.; Lu, L.; Currier, B. L.; Mikos, A. G.; Yaszemski, M. J. In *Tissue Engineering in Musculoskeletal Clinical Practice*; Sandell, L. J., Grodzinsky, A. J., Eds.; American Academy of Orthopaedic Surgeons: Rosemont, IL, 2004; Chapter 32.
(8) Jeong, B.; Bae, Y. H.; Kim, S. W. *J. Biomed. Mater. Res.* **2000**, *50*, 171.
(9) Jeong, B.; Bae, Y. H.; Kim, S. W. *J. Controlled Release* **2000**, *63*, 155.
(10) Lee, K. Y.; Alsberg, E.; Mooney, D. J. *J. Biomed. Mater. Res.* **2001**, *56*, 228.
(11) Payne, R. G.; Yaszemski, M. J.; Yasko, A. W.; Mikos, A. G. *Biomaterials* **2002**, *23*, 4359.
(12) Behravesh, E.; Jo, S.; Zygourakis, K.; Mikos, A. G. *Biomacromolecules* **2002**, *3*, 374.
(13) Shin, H.; Jo, S.; Mikos, A. G. *J. Biomed. Mater. Res.* **2002**, *61*, 169.
(14) Wang, D. A.; Williams, C. G.; Li, Q. A.; Sharma, B.; Elisseeff, J. H. *Biomaterials* **2003**, *24*, 3969.
(15) Elisseeff, J.; Anseth, K. S.; Simms, D.; McIntosh, W.; Randolph, M.; Langer, R. *Proc. Natl. Acad. Sci. U.S.A.* **1999**, *96*, 3104.
(16) Bryant, S. J.; Nuttelman, C. R.; Anseth, K. S. *Biomed. Sci. Instrum.* **1999**, *35*, 309.
(17) Bryant, S. J.; Anseth, K. S. *J. Biomed. Mater. Res.* **2001**, *59*, 63.
(18) Bryant, S. J.; Anseth, K. S. *Biomaterials* **2001**, *22*, 619.
(19) Bryant, S. J.; Anseth, K. S. *J. Biomed. Mater. Res.* **2003**, *64*, 70.
(20) Jabbari, E.; He, X. In *Advances in Bionanotechnology*; Peppas, N. A., Hilt, J. Z., Eds.; American Institute of Chemical Engineers: New York, 2005; p 92.
(21) Jabbari, E.; He, X. *Polym. Prepr.* **2006**, *47*, 353.
(22) Suggs, L. J.; Shive, M. S.; Garcia, C. A.; Anderson, J. M.; Mikos, A. G. *J. Biomed. Mater. Res.* **1999**, *46*, 22.
(23) Bryant, S. J.; Nuttelman, C. R.; Anseth, K. S. *J. Biomater. Sci., Polym. Ed.* **2000**, *11*, 439.
(24) Mi, F. L.; Tan, Y. C.; Liang, H. F.; Sung, H. W. *Biomaterials* **2002**, *23*, 181.
(25) Shin, H.; Temenoff, J. S.; Mikos, A. G. *Biomacromolecules* **2003**, *4*, 552.
(26) Schmedlen, K. H.; Masters, K. S.; West, J. L. *Biomaterials* **2002**, *23*, 4325.
(27) Park, Y. D.; Tirelli, N.; Hubbell, J. A. *Biomaterials* **2003**, *24*, 893.
(28) Dusek, K.; Prins, W. *Adv. Polym. Sci.* **1969**, *6*, 1.
(29) Weiss, N.; van Vliet, T.; Silberberg, A. *J. Polym. Sci., Polym. Phys. Ed.* **1979**, *17*, 2229.
(30) Janas, V. F.; Rodriguez, F.; Cohen, C. *Macromolecules* **1980**, *13*, 977.
(31) Hsu, T. P.; Ma, D. S.; Cohen, C. *Polymer* **1983**, *24*, 1273.
(32) Tobita, H.; Hamielec, A. E. *Polymer* **1990**, *31*, 1546.
(33) Matsuo, E. S.; Orkisz, M.; Sun, S. T.; Li, Y.; Tanaka, T. *Macromolecules* **1994**, *27*, 6791.
(34) Naghash, H. J.; Okay, O. *J. Appl. Polym. Sci.* **1996**, *60*, 971.
(35) Trompette, J. L.; Fabregue, E.; Cassanas, G. *J. Polym. Sci., Part B: Polym. Phys.* **1997**, *35*, 2535.
(36) Gurtovenko, A. A.; Gotlib, Yu. *J. Chem. Phys.* **2001**, *115*, 6785.
(37) Fuxman, A. M.; McAuley, K. B.; Schreiner, L. J. *Macromol. Theory Simul.* **2003**, *12*, 647.
(38) Calvet, D.; Wong, J. Y.; Giasson, S. *Macromolecules* **2004**, *37*, 7762.
(39) Winter, H. H.; Chambon, F. *J. Rheol.* **1986**, *30*, 367.
(40) Chambon, F.; Winter, H. H. *J. Rheol.* **1987**, *3*, 683.
(41) Ferry, J. D. *Viscoelastic Properties of Polymers*, 3rd ed.; Wiley: New York, 1980.
(42) Bhanu, V. A.; Kishore, K. *Chem. Rev.* **1991**, *91*, 99.

BM060648P